Vector acoustic intensity around a tuning fork

Daniel A. Russell[a)]
Graduate Program in Acoustics, The Pennsylvania State University, University Park, Pennsylvania 16802

Justin Junell[b)] and Daniel O. Ludwigsen
Physics Department, Kettering University, Flint, Michigan 48504

(Received 4 March 2012; accepted 15 November 2012)

The acoustic intensity vector field around a tuning fork is investigated. Theory for a longitudinal quadrupole source predicts a well-defined transition between near-field and far-field, with significant circulation of sound energy in the near-field. Vector components of the time-averaged intensity were measured using a two-microphone intensity probe and found to agree well with predictions from theory. The vector intensity map is interpreted, and shown to provide useful information about the near-field of an acoustic source.
[http://dx.doi.org/10.1119/1.4769784]

I. INTRODUCTION

The tuning fork is a simple apparatus that provides a wealth of information about acoustic sources including a nonharmonic frequency spectrum,[1,2] nonlinear generation of integer harmonics,[3] and an interesting radiated pressure field. In our previous paper,[4] we provided experimental evidence that a tuning fork vibrating in its fundamental mode behaves as a longitudinal quadrupole sound source, with a well-defined transition between near-field and far-field radiation patterns. Other less commonly observed vibrational modes were found to produce dipole and lateral quadrupole radiation patterns. Our experimental studies backed up the theoretical predictions of the radiated pressure field in an earlier paper by Sillitto.[5]

One of the interesting features of Sillitto's 1966 paper is that in addition to predicting the pressure field dependence on angle and distance, he also derived expressions for the acoustic intensity and predicted theoretical streamlines of the time-averaged acoustic energy flow around the fork. At the time when Sillitto's paper was published, experimental methods for reliably measuring acoustic intensity did not exist. However, since the early 1980s, the techniques and instrumentation are now available to measure intensity directly.[6]

In this paper, we investigate the vector sound intensity around a tuning fork. We first review the theoretical predictions and then compare measured vector intensity to theory. Finally, we discuss the transition from near-field to far-field in the sound field radiated by the fork.

II. ACOUSTIC INTENSITY AROUND A TUNING FORK

When a tuning fork vibrates in its fundamental mode, the two tines oscillate back and forth symmetrically.[3,7] A tuning fork vibrating in its fundamental mode has been shown to radiate sound in a manner consistent with the near-field and far-field radiation patterns associated with a longitudinal quadrupole sound source.[4,5] Figure 1 shows the orientation of the four point sources comprising the longitudinal quadrupole model used in the following theoretical analysis, with r being the radial distance from the source and ϕ being the angle around the source measured from the axis of the longitudinal quadrupole in the counterclockwise direction. The pressure p radiated by a longitudinal quadrupole is[5,8,9]

$$p=\frac{Ak}{r^3}[(3\cos^2\phi-1)(1+jkr)-(kr)^2\cos^2\phi]e^{j(\omega t-kr)}, \quad (1)$$

where $j=\sqrt{-1}$, k is the acoustic wavenumber ($k=2\pi/\lambda$, with λ being the wavelength), and $\omega=2\pi f$ is the angular frequency. The quantity A is an amplitude factor that depends on the strength, frequency, and dimensions of the quadrupole source.

As this pressure sound wave radiates away from the source it carries energy. Acoustic intensity is a measure of the flow of the acoustic energy per unit time per unit area carried by the sound wave radiated by a source. Intensity is defined as the product of the sound pressure p and the particle velocity $\vec{u}$ in the medium through which the sound wave is traveling[10]

$$\vec{I}(t)=p(t)\vec{u}(t), \quad (2)$$

where the arrows indicate that intensity and particle velocity are vector quantities. Most of the time, one is interested in the net flow of energy as represented by the time-averaged intensity[11,12]

$$\vec{I}=\frac{1}{2}\mathrm{Re}\{p\vec{u}^*\}, \quad (3)$$

where * indicates the complex conjugate and Re indicates taking the real part of the product.

The particle velocity $\vec{u}$ is related to the sound pressure through the conservation of momentum by Euler's equation[13]

$$\rho\frac{\partial\vec{u}}{\partial t}=-\nabla p. \quad (4)$$

In polar coordinates this becomes

$$\rho\frac{\partial\vec{u}}{\partial t}=-\frac{\partial p}{\partial r}\hat{r}-\frac{1}{r}\frac{\partial p}{\partial\phi}\hat{\phi}, \quad (5)$$

where $\hat{r}$ and $\hat{\phi}$ represent the unit vectors in the radial and counterclockwise angular directions, respectively. After taking the gradient of the pressure and then integrating with respect to time, the radial and tangential components of the particle velocity are found to be

$$u_r=\frac{e^{jkr}}{r^4}[(9\cos^2\phi-9)(1+jkr)-k^2r^2(4\cos^2\phi-1) - jk^3r^3\cos^2\phi], \quad (6)$$

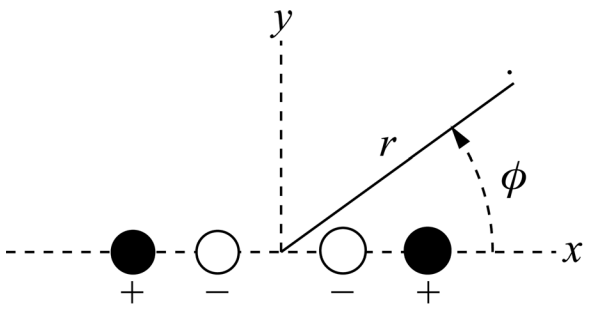

Fig. 1. Orientation of a longitudinal quadrupole source.

$$u_\phi = \frac{6k}{r^2}\left(\frac{k^2}{3} - \frac{1}{r^2} - \frac{jk}{r}\right)\cos\phi\sin\phi. \tag{7}$$

Multiplying the pressure from Eq. (1) by the complex conjugate of the components of the particle velocity from Eqs. (6) and (7) and taking the real part of the result, one obtains the vector components of the time-averaged intensity

$$I_r = \frac{1 - 3\cos^2\phi + (kr)^2\cos^4\phi}{r^2(kr)^2}, \tag{8}$$

$$I_\phi = -\frac{\sin(2\phi)}{r^2(kr)^2}. \tag{9}$$

The radial and tangential components of the intensity may be mapped to rectangular components for plotting purposes by using the geometric transformations

$$I_x = I_r\cos\phi - I_\phi\sin\phi, \tag{10}$$

$$I_y = I_r\sin\phi + I_\phi\cos\phi. \tag{11}$$

Figure 2 shows the "normalized" time-averaged intensity vectors in one quadrant of the xy-plane into which a longitudinal quadrupole source radiates sound, as predicted by Eqs. (10) and (11) for a frequency of 421 Hz. The vector plot was generated from the x and y components of the intensity using the VectorPlot function in *Mathematica*.[14] The lengths of the intensity vectors have all been drawn the same in order to emphasize the directional nature of the intensity field. Without this "normalization," the magnitudes of the intensity vectors in the far-field are too small to detect, due to the $1/r^4$ dependence of amplitude on distance. The axis of the longitudinal quadrupole source of Fig. 1 is aligned with the x-axis of Fig. 2.

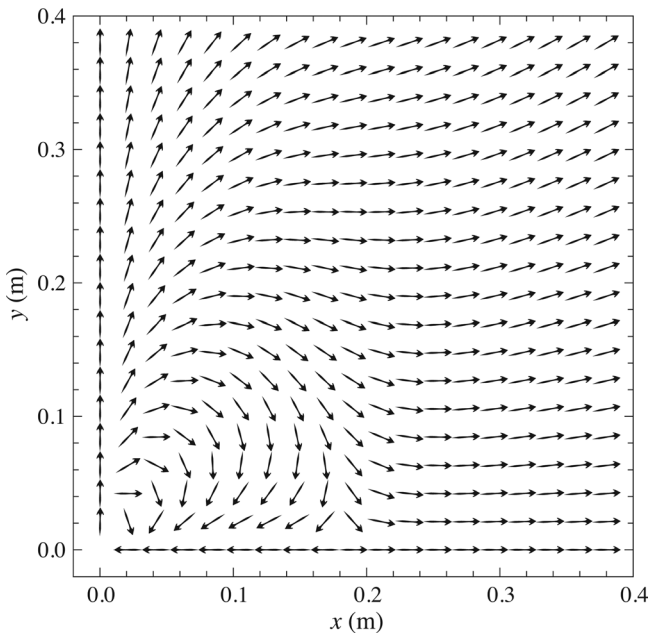

Fig. 2. Theoretical prediction of the "normalized" time-averaged acoustic intensity vectors in one quadrant around a longitudinal quadrupole source of frequency 421 Hz at the origin and aligned with the x-axis.

Several interesting features are apparent from the vector plot of time-averaged intensity predicted in Fig. 2. Along the y-axis of the plot, in a direction perpendicular to the plane of the fork tines, the time-averaged intensity is directed outward away from the fork at all distances. However, along the x-direction, in the plane of the fork tines, the time-averaged intensity points toward the fork tines for distances closer than 0.18 m but changes direction to point outward away from the fork tines at larger distances. The rest of the plot shows significant circulation of intensity, with the intensity in this quadrant circling around clockwise for distances closer than 0.18 m, but pointing mostly outward away from the fork at larger distances. The intensity field is symmetric and can be easily mirrored to the other three quadrants.

It is worth repeating that the time-averaged intensity represents the *net* flow of energy radiated by the tuning fork, averaged over one complete cycle of the fork oscillation. Therefore, the vectors in Fig. 2 do not change as the fork tines oscillate.

Along the x-axis, parallel to the fork tines in Fig. 2, there is a location at approximately 18 cm from the center of the fork where the intensity vanishes, pointing inward toward the fork tines for closer distances and outward away from the fork tines for larger distances. The theory for the radial component of the intensity from Eq. (8) predicts that the intensity will vanish at a distance equal to $\lambda/(\pi\sqrt{2})$, which for a 421 Hz source is 18.3 cm.

It should be noted, however, that while the time-averaged intensity vanishes at this point, the pressure due to the sound wave does not vanish. If the fork is held at a distance of 18 cm from the ear, one can very easily hear the sound pressure radiated by the tuning fork. Intensity is the product of pressure and particle velocity and indicates the direction of energy flow; the ear responds simply to the pressure amplitude of the sound wave and the pressure does not vanish at this location.

III. MEASUREMENTS OF ACOUSTIC INTENSITY

A. The two-microphone technique

To measure the time-averaged intensity around the tuning fork we used an intensity probe consisting of two identical phase-matched half-inch-diameter microphones, facing each other and separated by a fixed distance.[15] This type of intensity probe is often referred to as a p-p probe, because it calculates the intensity from two pressure measurements.

The two-microphone technique requires a finite difference approximation of the conservation of momentum in Eq. (4) to express the particle velocity in terms of the pressure gradient between the two microphones

$$u \approx \frac{j}{\omega\rho\triangle r}(p_b - p_a), \tag{12}$$

where p_a and p_b are the two pressure readings, $\triangle r$ is the spacing between the microphones, ρ is the density of the air, and ω is the angular frequency of the signal, in this case the frequency of the tuning fork. The intensity in Eq. (3) then becomes

$$I(\omega) = \frac{1}{2}\mathrm{Re}\left\{\frac{p_a + p_b}{2}\left[\frac{j}{\omega\rho\triangle r}(p_b - p_a)\right]^*\right\}. \tag{13}$$

The pressure gradient ensures that the intensity measurement will include a directional component; the intensity will be positive or negative depending on which microphone measures a higher pressure value. Multiplying the terms yields

$$I(\omega) = \frac{1}{2}\mathrm{Re}\left\{\frac{-j}{2\omega\rho\triangle r}[p_a p_b^* - p_b p_a^*]\right\}, \tag{14}$$

where we have ignored the auto-power spectra terms $p_b p_b^*$ and $p_a p_a^*$ because they are real quantities and don't contribute to the real part of the final time-averaged intensity.[16] The difference between products of the pressures can be written in terms of the imaginary part of the product

$$p_a p_b^* - p_b p_a^* = 2j\mathrm{Im}\{p_a p_b^*\}, \tag{15}$$

so that the intensity can be written in terms of the imaginary part of the product of the pressures

$$I(\omega) = \frac{\mathrm{Im}\{p_a p_b^*\}}{2\omega\rho\triangle r}. \tag{16}$$

If the pressure signals are recorded as frequency spectra using a two-channel FFT analyzer, then one can calculate the cross-spectrum[12,16]

$$G_{ab} = \frac{1}{2}[X_a^*(\omega)X_b(\omega)], \tag{17}$$

where X_a and X_b represent the two frequency spectra. Therefore, the time-averaged intensity can be obtained with a two-microphone probe from the imaginary part of the cross spectrum of the two pressure signals

$$I(\omega) = \frac{\mathrm{Im}\{G_{ab}\}}{\omega\rho\triangle r}. \tag{18}$$

B. Experimental setup

A 426.6 Hz tuning fork (with tines 1.3-cm thick, 0.9-cm wide, and 2.1-cm apart) was mounted in a stand with the stem clamped. A small, 1.0-g NiFeB magnet was attached at approximately the midpoint along the length on the outer surface of each tine. An electromagnetic coil was placed over one of the magnets, with the second magnet acting to evenly distribute the mass-loading. The fork was driven at its experimentally determined mass-loaded resonance frequency of 421.1 Hz. The tuning fork and driving coil were placed on a rotating turntable with the long axis of the tuning fork centered vertically on the turntable, and with both fork and coil isolated from the turntable by a foam pad. The intensity probe was positioned at a fixed distance from the center of the fork, with the microphones centered approximately 1 cm below the tip of the fork tines, as shown in Fig. 3. The outputs of the two microphones were recorded using a two-channel FFT analyzer. The turntable made one complete revolution every 80 s. A total of 320 measurements were collected for one complete rotation using the waterfall setting on the analyzer, with a 125 ms time average, and skipping every second record.

Intensity was measured at 2-cm increments from a distance of 9 cm from the central axis of the tuning fork (the closest possible center-to-center distance between probe and fork) out to 33 cm. At each distance, the radial and tangential components of the intensity were recorded separately, due to

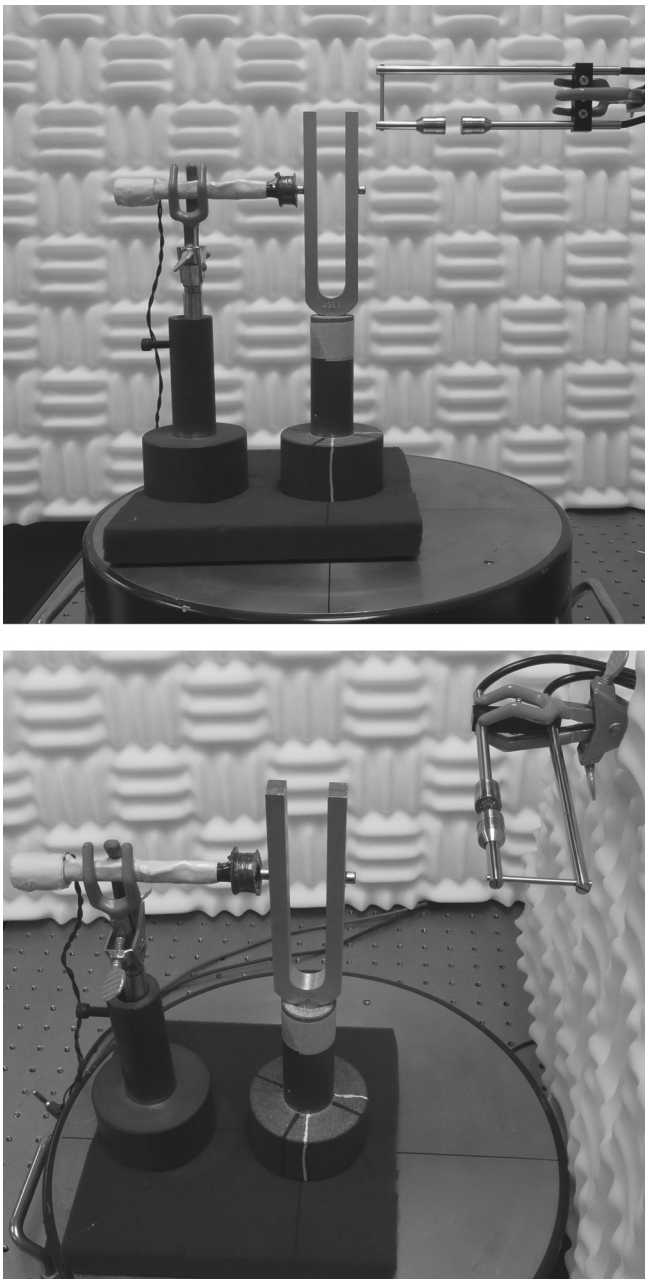

Fig. 3. Setup for measuring vector intensity around the tuning fork with a two-microphone probe in the radial direction (top) and in the tangential direction (bottom).

the need to rotate the probe by 90°, as shown in Fig. 3. A LabVIEW program was written to synchronize the intensity data for the two components. Values for the radial and tangential intensity vector components were then extracted by keeping every fifth data point, corresponding to a measurement every 5.6°around the circle. The sign of the tangential components was reversed to account for the relative motion between fork and probe; the turntable rotated the fork counterclockwise in front of a stationary probe, rather than the probe rotating around a stationary fork. The polar vector components of intensity were then translated to rectangular components for plotting with the ListVectorPlot function in *Mathematica*.

C. Discussion of results

Figure 4 shows the measured vector intensity in one quadrant around the tuning fork. As with Fig. 2, the vectors were "normalized" by drawing them all the same length to emphasize the directional nature of the intensity field. The black rectangles in the lower left corner of the figure represent the dimensions of the fork tines to scale. The general features of the measured data in Fig. 4 show very good agreement with the theoretical prediction in Fig. 2. In the far-field, the time-averaged intensity vectors essentially point outward, away from the fork at all locations. In the near-field, the time-averaged intensity points away from the fork along the y-axis in a direction perpendicular to the plane of the tines, but circulates around clockwise to point inward toward the fork along the x-axis parallel to the plane of the tines. The fact that the intensity vectors along the x-axis are not exactly parallel to the axis is likely due to the fact that the intensity measurements were averaged over 125 ms while the turntable was rotating, so a small tangential component shows up where there should be none.

A more noticeable difference between theory and results is the location along the x-axis where the time-averaged intensity changes direction. Theory predicts that for a 421 Hz source the change should occur at approximately 18 cm from the source, while Fig. 4 shows that the actual location is closer to 16 cm. Figure 5 compares the radial component of the time-averaged intensity as predicted from Eq. (8) for $\phi = 0$, along the x-axis parallel to the plane of the fork tines, to experimentally measured values. At large distances, the experimental data and theory agree very well. Differences between data and theory become apparent in the transition between near-field and far-field. The reason for this discrepancy is most likely due to the fact that the longitudinal quadrupole model treats the tuning fork tines as spherical point sources when the tines are really more like cantilever beams with a transverse size of about 1 cm and a length of 13 cm. It is interesting to note that a finite element computer model of the tuning fork intensity, which models the fork tines as two colinear dipole sources radiating into a two-dimensional plane, predicts the turning point along the x-axis to occur at a distance of 13.5 cm.[17]

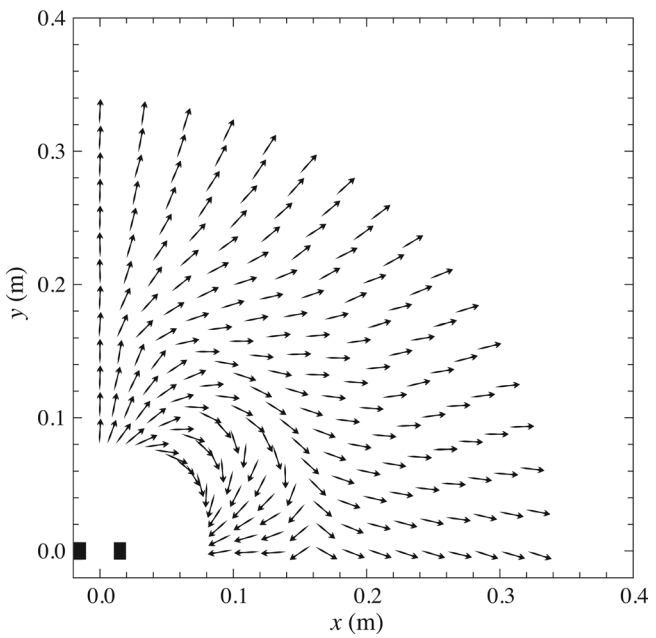

Fig. 4. Measurement of the time-averaged acoustic intensity in one quadrant around the tuning fork. Intensity vectors have been "normalized" in length.

IV. TRANSITION FROM NEAR-FIELD TO FAR-FIELD

This paper, together with our previous work,[4] effectively demonstrates that the sound field radiated by a tuning fork provides a very clear distinction between the near-field and far-field regions around a longitudinal quadrupole source. If the fork was a simple spherical source, the transition between near-field and far-field would occur at $kr = 1$, corresponding to a distance $r = 0.16\lambda$. In the near-field of a simple source, where $kr \ll 1$, the pressure and particle velocity are 90°out of phase and the complex radiation impedance is dominated by its imaginary part, indicating that the near-field primarily involves the local storage of energy in the elastic (potential energy) and inertia (kinetic energy) properties of the medium. In the far-field of a simple source, where $kr \gg 1$, the pressure and particle velocity are in phase and the complex radiation impedance is dominated by its real part, indicating that energy is carried away from the source by the outward propagating sound waves.

For a more complicated sound source like the tuning fork, which can be approximately modeled as a longitudinal quadrupole source, the transition from near-field to far-field occurs slightly farther from the source, at $r = 0.225\lambda$. However, the relationship between pressure and particle velocity, as well as the interpretations of radiation impedance, should be the same as for a simple source. The vector plots in Figs. 2 and 4 confirm the dominance of sound radiation in

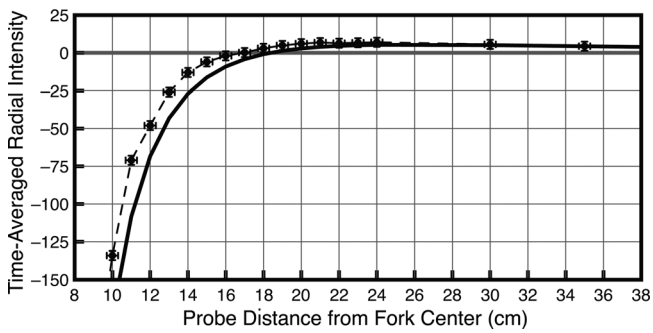

Fig. 5. Comparison between theory from Eq. (8) and experimental data for the radial component of the time-averaged intensity along the x-axis in the plane of the fork tines.

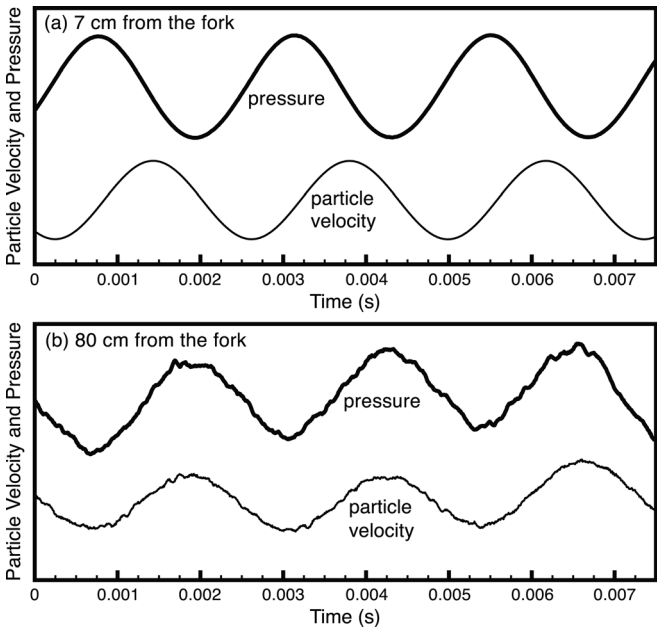

Fig. 6. Time signals for pressure (top traces) and particle velocity (bottom traces) measured with a Microflown *p-u* probe at distances of (a) 7 cm and (b) 80 cm along the *x*-axis in the plane of the fork tines.

the far-field and the local storage of energy, as evidenced by the circulation, in the near-field.

To confirm the relationships between pressure and particle velocity, these two quantities were measured simultaneously at various distances along the *x*-axis in the plane of the tuning fork tines using a Microflown USP match probe.[18,19] The Microflown, also known as a *p- u* probe, measures the pressure with a tiny microphone and the particle velocity with a MEMS hot-wire anemometer transducer. Figure 6 shows measured pressure (top traces) and particle velocity (bottom traces) at distances of 7 cm and 80 cm from the tuning fork, along the *x*-axis in the plane of the tuning fork tines. The distance of 7 cm is well within the near-field, and the measured pressure and particle velocity are clearly about 90° out of phase. At a distance of 80 cm, well into the far-field, the pressure and particle velocity are now in phase.

V. CONCLUSION

In this paper, we have provided experimental evidence to validate Sillitto's theoretical model of the vector intensity radiated by a vibrating tuning fork.[5] As was the case for directivity measurements,[4] the intensity data show a clear distinction between the near-field and far-field radiation regions. In the near-field, the time-averaged intensity predominantly swirls around the fork, proceeding outward from the perpendicular axis of the fork to circle around and point back inward toward the fork tines. In the far-field, the time-averaged intensity predominantly radiates outward away from the fork in all directions. At the transition between near-field and far-field, along the axis parallel to the fork tines, there is a location where the time-averaged intensity vanishes. Measurements of pressure and particle velocity in the near- and far-fields show the expected phase relationship, with *p* and *u* being 90° out of phase in the near-field and in phase in the far-field. The simple tuning fork is shown to provide a wealth of interesting information about acoustic sources and radiated sound fields.

ACKNOWLEDGMENTS

The first author appreciates the students who explored this experiment as a project during the years he taught PHYS-485, Acoustical Testing and Modeling, at Kettering University.[17] The authors are also grateful for the insightful suggestions from the two anonymous reviewers who critiqued this paper.

[a]Electronic mail:drussell@engr.psu.edu
[b]Currently with NASA

[1]A. Benade, *Fundamentals of Musical Acoustics*, 2nd revised ed. (Dover Publications, New York, 1990), pp. 40, 67.
[2]J. Backus, *The Acoustical Foundations of Music* (Norton, NY, 1969), p. 67.
[3]T. D. Rossing, D. A. Russell, and D. E. Brown, "On the acoustics of tuning forks," Am. J. Phys. **60**(7), 620–626 (1992).
[4]D. A. Russell, "On the sound field radiated by a tuning fork," Am. J. Phys. **68**(12), 1139–1145 (2000).
[5]R. M. Sillitto, "Angular distribution of the acoustic radiation from a tuning fork," Am. J. Phys. **34**(8), 639–644 (1966).
[6]F. J. Fahy, *Sound Intensity*, 2nd ed. (E&FN Spon, London, 1995).
[7]Dan Russell, "Tuning fork vibrations," <http://www.youtube.com/watch?v=AHXpJVSHwLc>.
[8]D. D. Reynolds, *Engineering Principles of Acoustics: Noise and Vibration Control* (Allyn & Bacon, Boston, 1982).
[9]A. D. Pierce, *Acoustics: An Introduction to Its Physical Principles and Applications* (Acoustical Society of America, Woodbury, NY, 1989), pp. 167–169.
[10]G. Rasmussen, "Intensity—Its measurement and uses," Sound Vib. **23**(3), 12–21 (1989).
[11]F. Jacobsen, "Sound Intensity," in *Springer Handbook of Acoustics*, edited by T. D. Rossing (Springer Science+Business Media, New York, 2007), pp. 1053–1075, Chap. 25.
[12]C. E. Wilson, *Noise Control: Measurement, Analysis, and Control of Sound and Vibration* (Krieger Publishing, Malabar, FL, 1994), pp. 31–32.
[13]L. E. Kinsler, *A. R. Frey, A. B. Coppens, and J. V. Sanders, Fundamentals of Acoustics*, 4th ed. (John Wiley & Sons, New York, 2000), pp. 117–119.
[14]Wolfram Research Inc., *Mathematica* 8.0, <http://www.wolfram.com>.
[15]"Instruments for the measurement of sound intensity," ANSI S1.9-1996 (American National Standards Institute, 1996).
[16]M. P. Waser and M. J. Crocker, "Introduction to the two-microphone cross-spectral method of determining sound intensity," Noise Control Eng. J. **22**(3), 76–85 (1984).
[17]D. A. Russell and D. O. Ludwigsen, "Acoustic testing and modeling: An advanced undergraduate laboratory," J. Acoust. Soc. Am. **131**(3), Pt. 2, 2515–2524 (2012).
[18]F. Jacobsen and H.-E. de Bree, "A comparison of two different sound intensity measurement principles," J. Acoust. Soc. Am. **118**(3), 1510–1517 (2005).
[19]Microflown Technologies <http://www.microflown.com/>.